Research on Controlling DC/AC Converter Using Solar Power System for The Applications in Industrial

Tran Duc Chuyen[*], Le Van Anh[#], Nguyen Cao Cuong[#], Nguyen Van Toan [#]

*#*Faculty of Electrical Engineering, University of Economics - Technology for Industries, Vietnam*

Abstract

This paper constructs a control structure to control a grid-coupled DC / AC converter capable of operating as required by a load-demand regulation program. This control structure consists of a current control loop on the inner ring and a power variable control loop on the outer ring. According to this structure, the internal loop controller uses a resonant controller with parameters defined in the frequency domain and a three-phase voltage reversible controller based on a control law that compensates the electrical components. Voltage so that the voltage characteristic; the current at the DC / AC converter output is always standard sinusoidal. Since then, a solar power source has been stored energy to supply the reverse console system and then supply it to the load consumption in civil and industrial. The article's research results on simulation and experiment have proven that this system is applied in systems exploiting renewable energy sources operating according to the requirements of the load demand regulation program.

Keywords: *Inverse controller, three-phase DC/AC power converter, power controller, power converter, Micro-grid, renewable energy source, solar power.*

I. INTRODUCTION

Today the exhaustion of natural fossil fuels; Oil, together with the greenhouse effect's influence, leads to an urgent need to build and use renewable energy. Thanks to the rapid development of power electronics; Solar and wind energy are becoming more popular among new renewable energy sources. These energy sources have replaced traditional fossil energy sources. This is a suitable choice for many countries worldwide [1, 3, 9].

Along with this development, load-on-demand management programs have also been developed to realize the redistribution of load demand and various sources' responsiveness throughout the system. At each node with the participation of renewable energy sources, power electronic converters such as DC / AC inverters play a very important role in power flow regulation and coupling grid [5, 6, 8, 13]. Simultaneously, renewable energy sources are often involved in generating the DC / AC converter's DC power side.

As in a number of domestic and foreign studies that have been studied, [10, 12] have not studied in depth from solar panels that are stored energy through the converter into the battery. It is then transferred to the controller,

inverter, and converter, which converts to the DC / AC voltage used in industrial loads at the factory where it is manufactured. Previous studies only stop at simulation but have not experimented with evaluating the power source's quality for the microgrid [14, 15].

This paper proposes a system to convert renewable electrical energy, from solar energy stored energy through a converter to the battery, then to the controller, inverter, converter, which converts voltage from DC / AC to industrial use (figure 1). The quality of the power and the power supplied to the load is always guaranteed by the power quality according to IEEE 519 power quality standards [2, 3, 16].
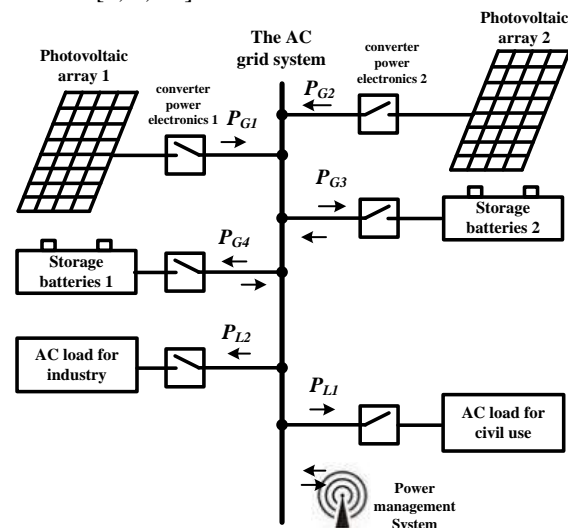

Fig 1: The Microgrid system main components

Energy systems are renewable energy sources such as (solar energy, photovoltaic array (PV), wind turbines, water, solar cells, etc.).

The energy collection/generation system is responsible for charging and storing energy when there is a surplus and discharging it when there are abnormal fluctuations in the grid. This can be done using solar cell array (photovoltaic array), batteries, supercapacitors or energy storage flywheel, etc.

Power electronic block is a power converter connected to the grid flexibly, including DC / AC converter, AC / DC, etc. This block can convert renewable energy into electricity with the right voltage, frequency, and phase angle to connect to the microgrid for power generation. For energy storage elements, electronic power blocks are capable of working in two directions, when the grid works

stably, the energy from the grid is stored in the storage element; when there is a sudden change in terms of voltage, energy from stored elements will be brought back to overcome fluctuations and stabilize the grid.

The grid system and consumption: Electricity after production, through the converter, is connected to the grid. From there, the electrical loads are provided by the grid's electricity.

There are also measurement and control units with executive functions; Manage the operation of the entire grid system such as power generation control, power electronic converter control, grid connection control, and charge/discharge control of the energy storage system [4, 6, 11, 14, 16].

II. THE BUILDING MODEL CONTROL SYSTEM THREE-LEVEL VOLTAGE SOURCE INVERTER

The main circuit of the neutral point clamped, grid-connected PV inverter is shown in Fig.2. In this figure: V_{dc} is DC voltage, C_1, C_2 are the capacitances of the DC side, L_f is the output filter inductance, R_f is the inductive filter resistance, is the filter capacitor, v_{a0}, v_{b0}, v_{c0}, are the output voltages of the C_f is the inverter component, I_{a0}, I_{b0}, I_{c0} are the output currents of the inverter device, Z_a, Z_b, Z_c, three-phase random loads, V_{al}, v_{bl}, v_{cl} are load voltages, and i_{al}, i_{bl}, i_{cl} are the currents flowing through the three-phase load, [3, 16].
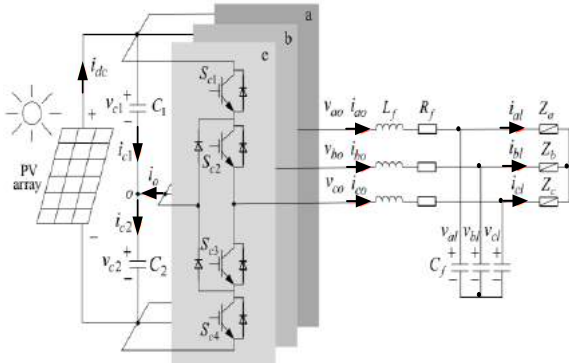

Fig 2: The topology diagram of a three-phase inverter for photovoltaic array systems
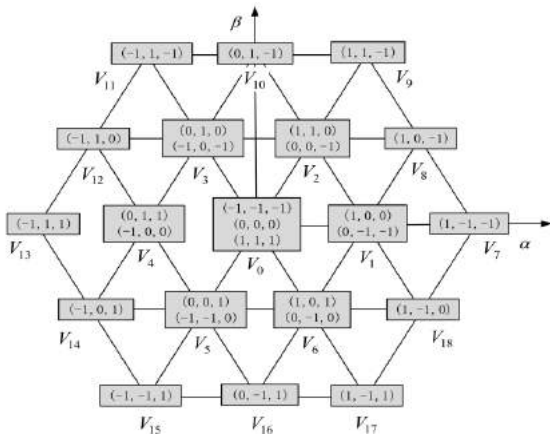

Fig 3: The relation between voltage vectors and switching states for a three-level inverter

A three-phase three-level neutral point clamped inverter can output three different voltage states in each leg, equal to ($V_{dc}/2$, 0, -$V_{dc}/2$) if each capacitor voltage is half of the DC-link voltage [1, 3]. Each leg's possible switching state can be denoted as (1, 0, -1). The corresponding relationship between the inverter voltage vector and the switch status is shown in Fig.2. The 27 possible switching states generate 19 nonredundant vectors in the $\alpha\beta$ frame.

According to Fig. 1, the dynamic model can be described using Kirchhoff's Voltage law as follows:

$$\begin{cases} L_f \dfrac{di_0}{dt} = v_0 - v_l - R_f i_0 \\ C_f \dfrac{dv}{dt} = i_l - i_0 \end{cases} \qquad (1)$$

which can be represented in a state-space equation of state follows:

$$\frac{dx}{dt} = Ax + Bu \qquad (2)$$

where component x, A, B is written as follows:

$$x = \begin{bmatrix} v_l \\ i_0 \end{bmatrix}, u = \begin{bmatrix} v_0 \\ i_l \end{bmatrix}, A = \begin{bmatrix} 0 & 1/C_f \\ -1/L_f & -R/L_f \end{bmatrix}, B = \begin{bmatrix} 0 & -1/C_f \\ 1/L_f & 0 \end{bmatrix} \quad (3)$$

A discrete-time representation of Equation (2) can be obtained as:

$$\begin{pmatrix} v_l(k+1) \\ i_0(k+1) \end{pmatrix} = G \begin{pmatrix} v_1(k) \\ i_0(k) \end{pmatrix} + H \begin{pmatrix} v_0(k) \\ i_l(k) \end{pmatrix} \qquad (4)$$

in which component G, H is written as follows:

$$G = e^{AT_s}, H = \int_0^{T_s} e^{A\tau} B d\tau \qquad (5)$$

wheres, T_s is the sampling time.

By using (2) and (5), the following equations can be derived:

$$G = \begin{pmatrix} g_{11} & g_{12} \\ g_{21} & g_{22} \end{pmatrix} = \begin{pmatrix} \cos q & p \sin q \\ (-1/p)\sin q & \cos q \end{pmatrix} \qquad (6)$$

$$H = \begin{pmatrix} h_{11} & h_{12} \\ h_{21} & h_{22} \end{pmatrix} = \begin{pmatrix} 1-\cos q & -p \sin q \\ (1/p)\sin q & 1-\cos q \end{pmatrix} \qquad (7)$$

wheres, $p = \sqrt{L_f / C_f}$, $q = T_s / \sqrt{L_f C_f}$

With Equation (3), the predicted load voltage can be expressed as:

$$v_l(k+1) = g_{11}v_l(k) + g_{12}i_0(k) + \\ + h_{11}v_0(k) + h_{12}v_l(k) \qquad (8)$$

Using the forward Euler approximation, the predicted value for the capacitor voltage at time instant k +1 is given by:

$$\begin{cases} v_{c1}(k+1) = v_{c1}(k) + \dfrac{T_s}{C} i_{c1}(k) \\ v_{c2}(k+1) = v_{c2}(k) + \dfrac{T_s}{C} i_{c2}(k) \end{cases} \qquad (9)$$

where $v_{c1}(k)$, $v_{c2}(k)$ are the sample value of the capacitor, and $i_{c1}(k)$, $i_{c2}(k)$ are current values flowing through the two capacitors in the present moment.

The values of $i_{c1}(k)$ and $i_{c2}(k)$ are relevant to the switch state, and they can be calculated as:

$$\begin{cases} i_{c1}(k)=i_{dc}(k)-\sum_{x=a,b,c} K_{1x}i_{x0}(k) \\ i_{c2}(k)=i_{dc}(k)-\sum_{x=a,b,c} K_{2x}i_{x0}(k) \end{cases} \quad (10)$$

Where, $K_{1x} = \begin{cases} 1, & if \ S_x = 1 \\ 0, & otherwise \end{cases}$, $K_{2x} = \begin{cases} 1, & if \ S_x = 1 \\ 0, & otherwise \end{cases}$

$x \in \{a,b,c\}$ represents a, b, and c three phases ($i_{dc}(k)$ is the current supplied by the voltage source V_{dc}.

Substituting Equation (10) into Equation (9), the predicted capacitor voltage in the DC link can be written as:

$$\begin{cases} v_{c1}(k+1)=v_{c1}(k)+\dfrac{T_s}{C}[i_{dc}(k)-\sum_{x=a,b,c} K_{1x}i_{x0}(k)] \\ v_{c2}(k+1)=v_{c2}(k)+\dfrac{T_s}{C}[i_{dc}(k)-\sum_{x=a,b,c} K_{1x}i_{x0}(k)] \end{cases} \quad (11)$$

The inverter model is used to predict the value of the load voltage in the next sampling interval for each of the different voltage vectors. The cost function considering voltage errors and balance in the DC link capacitor voltages is determined as:

$$g = \left| v_l^*(k+1) - v_l(k+1) \right| + \\ + \lambda_{dc} \left| v_{c1}(k+1) - v_{c2}(k+1) \right| \quad (12)$$

where $v_l^*(k+1)$ is the reference value of load voltage; λ_{dc} is the additional cost function element's weighing factor. The voltage vectors that minimize the cost function are selected, and the corresponding optimal switching state is generated. The Block diagram of the voltage control system for three-level inverters is shown in figure 4.
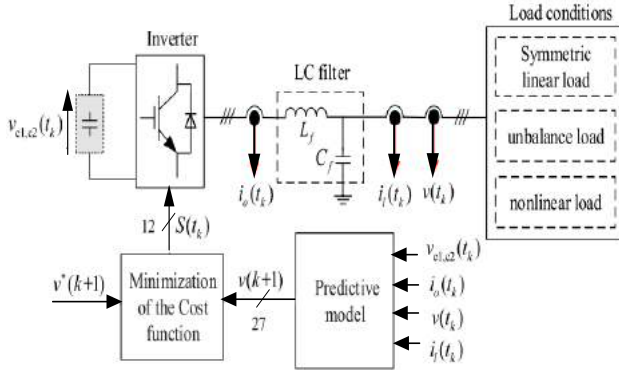

Fig 4: The block diagram of the voltage control system for three-level inverters

In this diagram fig.4, the structure diagram for controlling the industrial AC load system includes: from a solar cell system, through a converter with a single energy current, from which three frequency converters are fed phase, then to the filter system followed by the types of loads consumed.

III. THE SIMULATION AND EXPERIMENTAL

A. *The simulation*

At each sampling instant, the controller needs to evaluate the cost associated with a large variety of switching states [2, 3, 16].

As the controlled dynamics are fast, the computation delay can be significant compared to the desired closed-loop response [3, 4, 5, 6, 7].

A comparison between the actual condition and an ideal condition is shown in Fig.5, and the figure shows, τ is the calculation delay, v_l^* is the trajectory of the reference voltage. It can be seen that at a given time instant, all the possible switching combinations are evaluated with the information available at time t_k. Still, the control action is not applied at t_k because of the computation delay. As the control signal is determined with information measured at t_k but is applied at $t_k+ \tau$, the optimum switching state determined at t_k may not be the effective best solution. The voltage usually has some deviation from the desired reference.
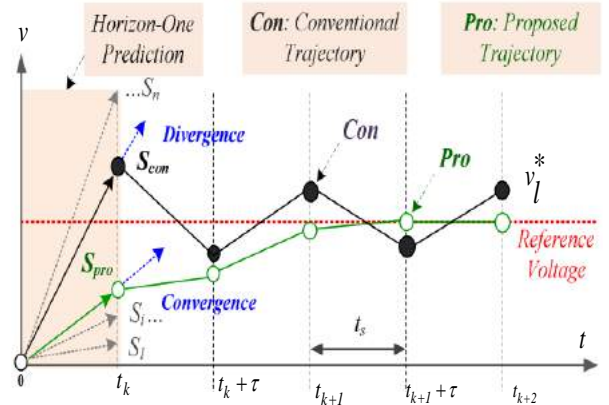

Fig 5: The comparison of tracking trajectory between actual and ideal conditions

In the proposed formulation, the time delay is explicitly considered, and the calculation is done considering the information measured up to time instant t_k defines the control action for t_{k+1}. In this approach, the control action used at t_k is the one determined at t_{k-1}. As in practice, the control action determined with the information up is determined at $t_k+ \tau$ it is applied to the plant input at t_{k+1}. As the control action imposed to the plant at t_{k+1} affects the plant output for time instants starting at t_{k+2}, the cost function considers the error values at t_{k+2} as:

$$g = \left| v_l^*(k+2) - v_l(k+2) \right| + \\ + \lambda \left| v_{c1}^*(k+1) - v_{c2}(k+2) \right| \quad (13)$$

The reference voltage can be expressed as:

$$v_l^*(k) = V_l^*(k).e^{2j\theta(k)} \quad (14)$$

where $V_l^*(k)$ is the amplitude of the voltage reference θ_k and is the vector angle of the voltage reference. In steady-state, the vector rotates with constant angular velocity ω, and the amplitude is constant. In this situation,

the voltage reference of time instant t_{k+2} can be expressed as a function of the information known at t_k as:

$$v_l^*(k) = V_l^*(k).e^{2j\omega T_s} \qquad (15)$$

To verify the effectiveness of the proposed control algorithm, the controller was evaluated using simulations. The sampling time $T_s = 22\mu s$ and the amplitude of the load voltage reference $v^* = 220\sqrt{2}$ are considered in simulations. The control system for three-level inverters with parameters is given in Table I. The following three different loading parameters are considered to validate the proposed control algorithm:

TABLE I: Parameters system for three-level inverters

| No	Variables	Description	Value
1	V_{dc}	DC link Voltage	700V
2	C_1, C_2	DC link capacitors	460µF
3	L_f	Filter inductance	2,5mH
4	R_f	Filter resistance	0,03Ω
5	C_f	Filter capacitor	100µF
6	U_{dc}	Voltage PV	60-150 VDC

With the load here is an industrial three - phase AC motor load with parameters: Three phase AC motor, P = 2,2kW, U = 380V, I = 8,6A, speed 1500 rpm, p = 2, motor is hard coupled to the load: dc generator: P = 4kW, U = 220V, I = 8,6A, speed 1750 rpm, frequency 50Hz.

From the controller simulation parameters proposed above, the authors have built a simulation model on the Matlab Simulink environment [3, 7] and obtained the following results:

Case 1: Simulation results with the voltage across the load; when the load changes, the voltage will not change significantly. From 0.1s to 0.12s, the current was almost unchanged in all three phases. When it was from 0.12s to 0.14s, the current changed markedly, as shown in figure 6.
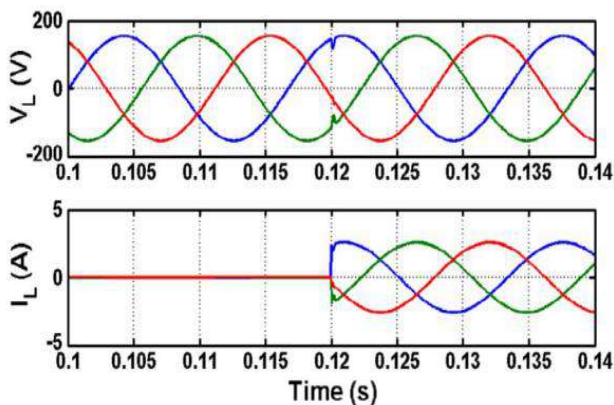
Fig 6: The simulation results when the load changes in case 1
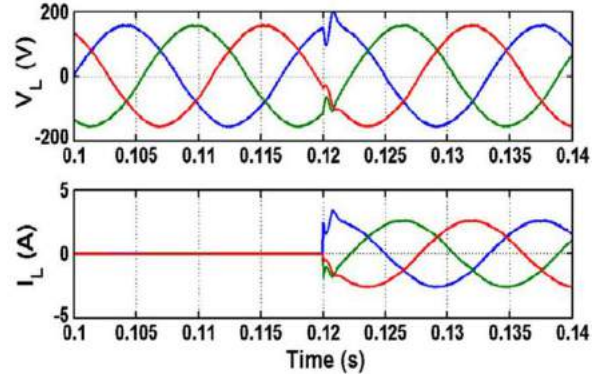
Fig 7: The simulation results when the load changes in case 2

Case 2: The simulation results with the voltage on the load at any time. When the load changes, the voltage changes no more than case 1. At the time of 0.1s to 0.12s current electricity was almost unchanged in all three phases. When it was from 0.12s to 0.14s, the current changed more significantly than in case 1. The results were shown in figure 7.

Case 3: when the motor rotates at the no-load three-phase voltage on load with simulation results, as shown in figure 8. The response time is 0.2s; the three-phase voltage always meets the standard of phases A, phase B, phase C. A good working control system can be applied in the industry.
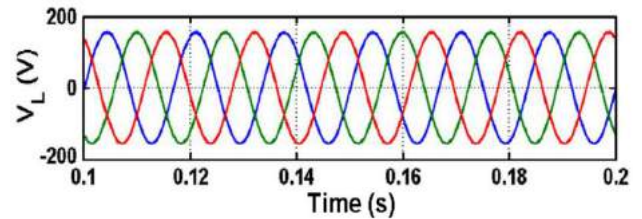
Fig 8: The Results of simulation of motor voltage without load consumption in case 3

Observing the results shows that when using the controller has been studied above, we see the sustainability; the stability of the control rule against the effects of an unknown component, the noise will change the transition time, increasing the fast impact of the control system; then the proposed algorithm is still working stably; The output voltage quality of the 3-phase inverter industrial load control is always stable and balanced, we say the system works stably. It can be seen that these new proposed studies have helped when the system does not have a 3-phase grid, but only the solar cell system is fed to the system. The system still provides 3-phase AC loads for industry work stably. Moreover, in the transient mode, the controller's response also compensates for the missing voltage components thanks to the capacitor system, the filter system, etc. They always do well and create quality sources. With high power, the system also responds to a relatively fast time.

B. The experimental

The Experimental study with a three-phase reverse flow system, as shown in figure 8, including The three-phase AC motor parameter, ise the same as in the simulations. The parameter table is as shown in Table 1. And devices located on inverted table: current transformer 50A / 5A, power module IGBT 25A / 1200V, digital control module dsPIC30F4011, display module LCD - ICEA, oscilloscope, power source transformer, etc. In addition, there are also a number of supporting devices such as power transformers, oscilloscopes, measuring devices, 1.5KW DC motor, DC voltage to create loads, and many other types of equipment for switching and other protection. The test system with inverters parameter table is as follows:
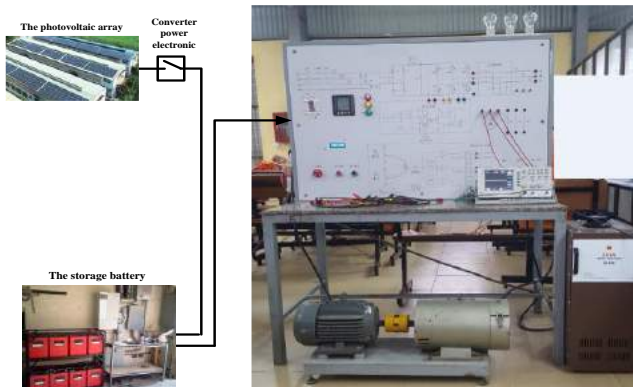
Fig 9: The image of the experimental structure of three-phase inverse flow in the reality

The control program combines real-time on Simulink with the three-phase DC / AC converter control system's console using solar power for industrial applications (figure 9). The experimental process calculates the converter's design, such as the inverted table system, from the input DC voltage taken from the energy cells passed through the converter and stored in the battery. Then power the inverse system, thanks to the converters, digital signal processors process the output signal, using the proposed control algorithm, then compensate the voltage components so that the voltage characteristics; the current at the DC / AC converter output is always standard sinusoidal. Meets power quality specifications such as IEEE519 for industrial and civil load control.
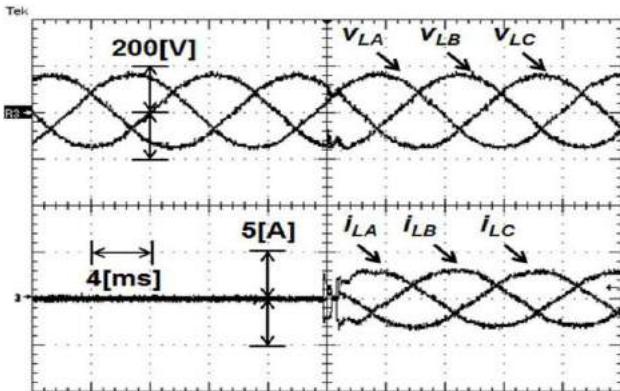
Fig 9: The three-phase voltage and current response as measured on an oscilloscope

Measured response to varying load voltages and currents measured from motor phases has proven that the system works well in simulation and real production. V_{LA}, V_{LB}, V_{LC} are the measured values of the voltage of phases A-B-C; the remaining phase currents i_{LA}, i_{LB}, i_{LC} are measured values of currents of phases A, B, C, always showing the correct process. The experimental results measured on the oscilloscope, compared with the simulation results and the experimental results show that the proposed controller works according to the requirements of the IEEE519 power quality. The system always works well in all different conditions. We say the system always works with a higher quality of control with different loads than the existing systems.

IV. CONCLUSIONS

In this paper, improving the quality of renewable energy in micro-grids cannot use simple control systems, so research on using the proposed controller to propose algorithms for some industrial control systems when using grid-connected solar power is facing a number of problems. Power quality problems. This research applies to control systems in the industry such as robotic systems, precise control systems for drug packaging machines in the pharmaceutical industry, CNC cutting machine control systems, weapons mounting systems. In the army, ... always ensures the quality of electricity according to national standards.

REFERENCES

[1] Nguyen Binh, Power electronics, Science and Technics Publishing House, Viet Nam, 2006.

[2] Vo Minh Chinh, Power electronics, Science and Technics Publishing House, Viet Nam, 2015.

[3] Tran Duc Chuyen, Tran Xuan Kien Power electronics and applications, Science and Technics Publishing House, Viet Nam, 2017.

[4] Nguyen Phung Quang and Jörg-Andreas Dittrich Intelligent electric drive, Science and Technics Publishing House, Viet Nam, 2006.

[5] Nguyen Doan Phuoc, The Advanced control theory, Science and Technics Publishing House, Viet Nam, 2015.

[6] Asif Sabanovic, Leonid M. Fridman and Sarah Spurgeon, Variable Structure Systems from principles to implementation, first published, 2004.

[7] László Keviczky, Ruth Bars, Jenő Hetthéssy, Csilla Bányász, Control Engineering: MATLAB Exercises, Publishing by Springer Nature Singapore Pte Ltd, USA ISSN 1439-2232, 2019.

[8] Andrea Bacciotti, Stability and Control of Linear Systems, Publishing Ltd; Springer Nature Switzerland AG 2019.

[9] Naser Mahdavi Tabatabaei, Ali Jafari Aghbolaghi, Nicu Bizon, Frede Blaabjerg Editors, Reactive Power Control in AC Power Systems, Springer International Publishing AG, 2017.

[10] Zafar Iqbal, Nadeem Javaid, Saleem Iqbal, Sheraz Aslam, Zahoor Ali Khan, Wadood Abdul, Ahmad Almogren, and Atif Alamri, A Domestic Microgrid with Optimized Home Energy, Management System, Energy, 11, 1002, ISSN: 0360-5442, 2018.

[11] B. Xiao, L. Hang, J. Mei, C. Riley, L. M. Tolbert, and B. Ozpineci, Modular cascaded H-bridge multilevel PV inverter with distributed

MPPT for grid-connected applications, IEEE Trans. Ind. Appl., vol. 21, no. 2, pp., 1722–1731, Mar 2015.

[12] Kaspars Kroics, Laila Zemite, Gatis Gaigals, Analysis of Advanced Inverter Topology for Renewable Energy Generation and Energy Storage Integration into AC Grid, Proceeding of 16th International Scientific Conference Engineering for Rural Development, ISSN: 1691-5976, 2017.

[13] Zafar Iqbal, Nadeem Javaid, Saleem Iqbal, Sheraz Aslam, Zahoor Ali Khan, Wadood Abdul, Ahmad Almogren, and Atif Alamri, A Domestic Microgrid with Optimized Home Energy Management System, Energy, 11, 1002, ISSN: 0360-5442, 2018.

[14] Teresa Orlowska - Kowalska, Frede Blaabjerg, Jose Rodriguez, Advanced and Intelligent Control in Power Electronics and Drives, Springer Publisher, ISSN 1860-9503, ISBN 978-3-319-03401-0, 2014.

[15] Ningyun Zhang, Houjun Tang and Chen Yao, A Systematic Method for Designing a PR Controller and Active Damping of the LCL Filter for Single-Phase Grid-Connected PV Inverters, Energies, ISSN 1996-1073, 7, 2014.

[16] The IEEE International Conference on Power and Energy (PECon20 10)., Nov 29 - Dec 1, 2010, Kuala Lumpur, Malaysia.